

Controlling pressure in microsystem packages by on-chip microdischarges between thin-film titanium electrodes

Scott A. Wright^{a)} and Yogesh B. Gianchandani

Department of Electrical Engineering and Computer Science, University of Michigan, Ann Arbor, Michigan 48109

(Received 14 May 2007; accepted 20 August 2007; published 21 September 2007)

This article describes on-chip sputter-ion pumps and their use in the controlled reduction of pressure in large cavity packages. The devices utilize thin-film titanium electrodes patterned on glass substrates and exposed to the cavity environments. Microdischarges between the electrodes sputter the cathodes, resulting in the selective chemisorption of oxygen, nitrogen, and other titanium-reactive gases. dc and pulsed high voltage powering schemes are investigated. Using dc discharges, devices on a 1 cm² footprint remove 168 Torr of air from a hermetically sealed commercial package with a volume of 6.33 cm³. Starting at 200 Torr, the removal rate of air is 7.2 Torr/h; for oxygen it is 11.5 Torr/h and for nitrogen 3.4 Torr/h. The relative humidity is reduced 6%/h, starting with 61%. The pumps have been shown not to remove helium from the environment. A 5× increase in pump power efficiency is obtained through the use of 25 ms pulsed discharges as opposed to dc discharges. The gas removal rates also depend on both initial pressure and discharge gap spacing. A theoretical model outlining the dependency of gas removal rates on microdischarge parameters is reported.

© 2007 American Vacuum Society. [DOI: 10.1116/1.2782510]

I. INTRODUCTION

Vacuum-sealed cavities are essential for a variety of micromachined sensors and actuators. For example, resonating devices such as gyroscopes and frequency references utilize them to minimize damping; pressure sensors utilize them as references; and electrostatic actuators such as switches are packaged in them to minimize the likelihood of charge accumulation and corrosion. The absorption or removal of gas from these sealed cavities is used to lower the pressure below the initial sealing pressure or to maintain a desired pressure over extended time periods. This is necessary because as the cavity volume is scaled down, its internal pressure can be easily increased by even small amounts of parasitic leakage, such as outgassing from surfaces or diffusion of gases through the cavity walls. Removal of moisture and less reactive gases such as nitrogen can be particularly challenging.

Options for gas absorption or removal that eliminate moving parts are promising from the viewpoints of longevity and field usability. Coatings and pumps have been suggested for use on the microscale to evacuate small cavities. Past efforts involving the application of coatings to the inside of sealed cavities include nonevaporable getters, thin-film getters (e.g., Nanogetters™), and reactive sealing.^{1–4} While these technologies work on both the macroscopic and microscopic scales, they typically operate in the millitorr range and require activation temperatures of 200–550 °C. For example, nonevaporable SAES getters, such as an alloy of Zr–V–Fe, St 707, are used to maintain vacuum levels and must ideally be externally or locally activated at 450–500 °C.⁵ Micromachined thermal molecular pumps without moving parts have

been proposed, and Knudsen pumps have also been developed.^{6,7} However, these typically require high temperatures as well. For devices that require pressure control near their maximum operating temperature (typically 100–150 °C), alternative or complementary means of controlling the pressure are needed.

Titanium is used as a getter in macroscale capture pumps including titanium sublimation pumps (TSPs) and sputter-ion pumps (SIPs), which operate in high and ultrahigh vacuum environments. TSPs function by subliming a hot filament of titanium onto the inner walls of a chamber where it chemisorbs impinging reactive gases. Macroscale SIPs operate through the creation of discharges in externally applied magnetic fields, which trap electrons and ionize the surrounding gases. Ions, which are then accelerated toward the cathodes, sputter fresh titanium onto the surrounding walls and anode. Titanium ions are known to getter both nitrogen and oxygen.^{8–12} Heavy nonreactive gases can also be confined as they are buried by the deposited materials.^{8–10}

The use of microdischarges in sputter-ion pumps is appealing because the discharges are very localized (to <500 μm) and allow air removal at room temperature and atmospheric pressure. The sputtering performed by microdischarges has previously been used to synthesize thin films through cluster-beam deposition.¹³ In addition, a microscale pump has been developed, which utilizes an electron-generating cathode to impart motion to air for the purpose of cooling electronics, as opposed to removing pressure from a sealed cavity.¹⁴

This article describes titanium microscale sputter-ion pumps (micro-SIPs) without moving parts that can remove relatively large volumes of air from sealed cavities. (Portions of this article appear in conference abstract form in Ref. 15.)

^{a)}Author to whom correspondence should be addressed; electronic mail: scottwri@umich.edu

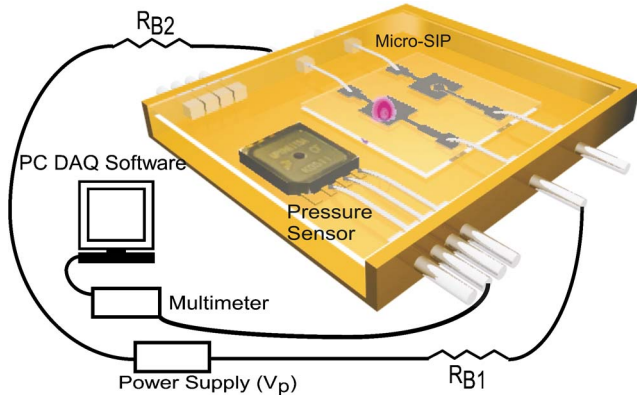


FIG. 1. Schematic of a commercial package, commercial pressure sensor, micro-SIP, power, and readout circuitry. R_{B1} and R_{B2} are ballast resistors of varied resistance which limit the current flowing between the anode and cathode.

Micro-SIPs operate in the manner of macroscale SIPs: They utilize microdischarges between thin-film titanium electrodes on a microchip to sputter a cathode and chemisorb gases through reactive sputtering. The amount of air removed is controlled through the duration of the applied voltages that energize the created microplasma discharges.

In addition to the evacuation of sealed cavities, this article explores the influence of (1) the micro-SIP design, (2) the environment in which micro-SIPs are operated, (3) the mode of micro-SIP operation, and (4) microdischarge characteristics on micro-SIP pumping operation. Microdischarges differ in some important ways from macroscale plasmas,^{16,17} which influences micro-SIP performance. For example, their ionization efficiency is typically low, the electron energy can exceed 100 eV, and they resemble negative glow discharges as they are driven primarily by secondary electron emissions from the cathode. Some of the discharge properties that impact micro-SIP performance are the secondary electron density and peak power, Townsend ionization coefficients, discharge characteristics, ionization efficiencies of various gases, and the composition of the exposed electrode pair surfaces. The study reported here explored these factors through examining the various micro-SIP discharge gap spacing at different pressures, the removal rate of various gases, humidity removal, and the ability of pulsed micro-SIP operation to improve efficiency through neutralizing positive surface charge buildup.

II. DEVICE CONCEPT AND OPERATION

The microchips that constitute micro-SIPs consist of one or more planar thin-film titanium anode-cathode pairs patterned on glass substrates separated by discharge gaps. They can be enclosed in hermetically sealed industry-standard packages and operated to remove air and humidity, as shown in Fig. 1. Microdischarges are created by applying voltages across the micro-SIP electrode pairs, and the cathodes are sputtered while chemisorbing select gases. Schematics displaying basic micro-SIP features are shown in Fig. 2. The micro-SIPs are designed with circular discharge gaps for uni-

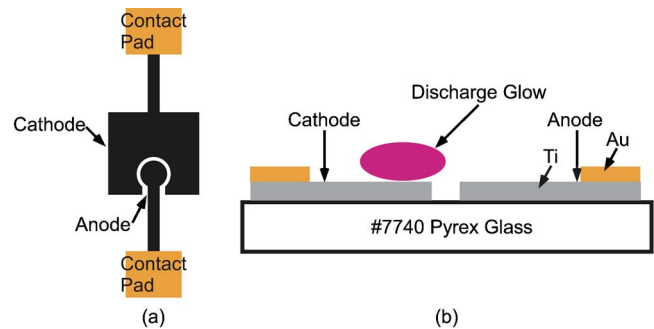


FIG. 2. Schematics of micro-SIP electrodes: (a) top view and (b) side view.

form sputtering and with large cathodes to increase the amount of available titanium. Increasing the voltage differences between micro-SIP electrodes increases the proportion of beam electrons with energies above 100 eV.¹⁷ Beam electrons are electrons emitted from the cathode, which travel without collisions through the cathode sheath while attaining high energies and eventually ionizing atoms. For this reason, relatively high voltages of 1000–1500 V are applied to operate the micro-SIPs. Power is applied through cavity leads (or, alternatively, by adjacent circuits that are copackaged with them). Given that typical microelectronic devices operate with low voltages ($< \sim 10$ V), separate circuits and isolation are required to provide the high voltages required to operate micro-SIPs. Typically, 20 μm of polyimide provides sufficient insulation for this.¹⁸ External ballast resistors are used in series with the electrodes to limit the current and provide control over discharge energy. The sputtered ions from micro-SIPs should not affect surrounding micromachined devices at higher pressures due to their low mean free path. At lower pressures, micro-SIPs can be enclosed in separate wells to block sputtered ions, a concept similar to the walls used in macroscale SIPs to block ions from sensitive structures.

Micro-SIPs function in a manner similar to traditional SIPs, operating by reactively sputtering titanium targets, but there are several differences as well. Macroscale SIPs create plasma regions between the anodes and cathodes while using external magnets to spatially confine the carriers. In contrast, microscale plasmas do not require magnetic confinement, as past work shows that discharges between narrowly spaced electrodes can be spatially confined in a very effective manner by controlling the powering scheme.^{18–20} In addition, stable microplasma discharges can be created, and reactive sputtering can occur at pressures as high as atmospheric pressure through the creation of very localized microplasmas, without creating unstable arc discharges.²¹ This is a result of “ pd scaling,” in which using small distances (d) between electrodes at atmospheric pressure (p) allows low breakdown voltages and results in lower current densities. At 760 Torr, the minimum breakdown voltage in air is achieved with an ~ 8 μm gap. This causes the breakdown voltages at high pressures, when using very small gaps, to be similar to those found in large volume, low-pressure plasmas. A dis-

charge gap distance less than 1 mm is required to approach the minima in Paschen's curve for almost all gases at atmospheric pressure.²²

Titanium has been shown to getter CO, CO₂, H₂, N₂, and O₂ with high efficiency in SIPs and in the more general category of getter-ion pumps.¹¹ It also reacts with water vapor to form oxides and liberate hydrogen in these getter-ion pumps.⁹ In macroscale titanium SIPs the deposited film layers, when removing air, have been shown to consist of 44% Ti, 40% N, 8% O, and 8% C.²³ Titanium and nitrogen are known to be uniformly distributed throughout the thickness of the deposited layer as well. These data indicate that one titanium atom is able to getter approximately one atom from the surrounding air environment.¹² However, microscale discharges differ in some ways, which can potentially change this.¹⁶ In particular, they are typically localized above the cathode, which can affect the redeposition pattern of sputtered molecules and, consequently, the final distribution of compounds. In addition, microdischarges have electrons and ions with extremely high energy, which can affect the binding of titanium with gas molecules.

In summary, like their larger-scale counterparts, microscale titanium sputter-ion pumps operate by chemisorbing gases from the environment. The devices differ in their size, the need for magnetic confinement, and useful operating range because micro-SIPs present localized plasmas at atmospheric pressure.

III. DESIGN AND FABRICATION

The micro-SIPs are designed with the intent of maintaining controlled, progressive cathode sputtering for extended durations of time. To accomplish this, the cathodes are designed to erode evenly along the discharge gap boundaries by surrounding the circular anodes with the cathodes. Finite element analysis (FEA) confirms that the circular design provides a uniform electric field over a large boundary of interaction between the micro-SIP electrode pairs. In contrast, if any sharp corners are present, the discharges would form at these locations preferentially. Three different micro-SIP designs for prolonged reactive sputtering are fabricated on separate chips, each with a 1 cm² footprint. The first micro-SIP design (version 1) has two single anode/cathode pairs and uses separate lead connections for each electrode, providing redundancy should one electrode be destroyed through the application of a large current or a bad connection. The second micro-SIP design (version 2) [Fig. 3(a)] has a single composite anode that interacts with eight separate but identical cathodes. As anodes are not significantly sputtered by the discharge, a common lead to them is sufficient. Each cathode can be activated individually or shunted off-chip with others. In this design, four times as much titanium is available for reactive sputtering as compared to version 1. The third micro-SIP design (version 3) [Fig. 3(b)] has a single anode and two cathodes. Each cathode has 15 discharge gaps, which maximize the amount of potentially sputtered titanium but version 3 does not allow the user as much

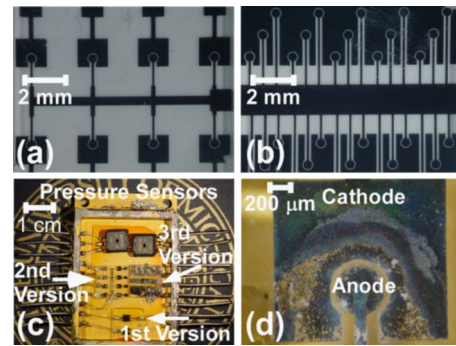


FIG. 3. (a) Version 2 chip with a single anode and eight cathodes. (b) Version 3 chip with a single anode and two cathodes, each having 15 discharge gaps. (c) A commercial package after opening, with two commercial pressure sensors and three different micro-SIP versions. (d) Micro-SIP electrodes displaying remains of a cathode after reactive sputtering, illustrating areas of complete titanium sputtering.

control compared to the other versions. Versions 1, 2, and 3 have 5.06, 1.82, and 33 mm² cathodes, respectively. Figure 3(c) illustrates the packaged devices.

In addition to the devices described above, additional version 2 micro-SIPs with identical cathode areas of 1.82 mm² and discharge gap spacing of 35, 50, 75, 100, and 150 μm were fabricated to evaluate the relationship between gas removal rate and discharge gap spacing. Despite the larger gaps, at atmospheric pressure the breakdown voltages of these micro-SIP electrode pairs is theoretically estimated to be between 500 and 1200 V.²⁴

All micro-SIPs were fabricated with two masks to simplify processing. A Ti film (1 μm thick) and a Au film (500 nm thick) were thermally evaporated onto No. 7740 Pyrex™ glass wafers (500 μm thick) without removing the wafers from vacuum. The contact pads were patterned on the gold layer using photolithography and etched using Transene GE-8148 gold etchant, which does not etch titanium. The electrodes were then patterned in the titanium layer using photolithography to produce the patterns shown in Figs. 3(a) and 3(b).

IV. THEORETICAL CONSIDERATIONS

The gas removal rate achieved by micro-SIPs depends on a number of design and operating parameters, such as electrode shape, spacing, material, discharge energy, and ambient pressure. In particular, the ambient pressure has been shown to affect microdischarges. Past reports have established through modeling that in microdischarges created in cylindrical metal-dielectric-metal sandwich structures in argon, with 200 μm discharge gaps and 100 μm thick electrodes, electron density surrounding the cathode increases monotonically between 50 and 625 Torr due to more tightly confined secondary electrons.¹⁷ Ionization and the density of atoms in excited states have also been shown to increase approximately linearly with pressure in this range as a result of an increase in secondary electron peak power and an increase in current density. This indicates that increasing the pressure causes an increase in electron density, ionization, and sec-

ondary electron peak power, which theoretically contribute to an increase in sputtering rates and the resulting micro-SIP air removal rates. However, this previously developed model did not explore sputtering in relation to microdischarges.

The theoretical increase in ionization and secondary electron production with decreasing discharge gap spacing should cause micro-SIPs with smaller discharge gaps to function more effectively. The electron ionization coefficients characterize the rate of electron impact ionization and the discharge itself, as dc discharges are sustained by electron movement in space. The first Townsend ionization coefficient α indicates the number of electron-ion pairs created per unit distance, while the secondary ionization coefficient γ represents the fraction of primary ionizing collisions that result in additional secondary electron production. The attachment coefficient a represents the number of electrons which attach themselves to electronegative molecules per unit distance and reduces the effective first ionization coefficient $\alpha_{\text{eff}} = \alpha - a$. These coefficients are influenced by the discharge gap spacing between electrodes and affect the gas removal rates of micro-SIPs. The ratios of electric field strengths to pressure (E/p) obtained in micro-SIPs between 100 and 760 Torr, 22–1071 V/(cm Torr), are similar to those obtained in macroscale plasmas due to the shorter discharge gap distances but higher operating pressures. The obtained E/p ratios are valid for sustained discharges as they exceed the threshold necessary to keep the attachment coefficient a less than α . If this threshold is not exceeded, the multiplication of electrons is impossible. The relatively small pd values indicate that avalanche multiplication, as opposed to the streamer mechanism, causes breakdown and, thus, that the Townsend mechanisms are valid. The streamer mechanism is a transient method of spark breakdown occurring at high pd values, in which thin ionized channels form between electrodes but are not sustained.²⁵

Both ionization coefficients of nitrogen increase as the discharge gap is reduced from 150 to 35 μm . The first ionization coefficient increases from 305 to 872 ion pairs/cm, while the second ionization coefficient γ increases from 1.09×10^{-8} to 4.99×10^{-6} with a 1500 V operating voltage at 100 Torr without considering attachment. A larger γ indicates more secondary electrons, making an increase in γ beneficial to microdischarges and micro-SIP operation as the discharges are primarily driven by secondary electron emission. However, γ is much smaller than in traditional plasmas due to the relatively small discharge gap spacing in all micro-SIPs. The greater amount of ionization and electron emission obtained using smaller discharge gaps becomes increasingly important as the ionized nitrogen mean free path decreases with increasing pressure, from 0.48 μm at 100 Torr to 0.063 μm at 760 Torr, and the microplasma becomes more confined. This is also consistent with the finding that discharges favor shorter path lengths at higher pressures.¹⁶

The characteristics of the discharges themselves also influence the gas removal rates of micro-SIPs. As the pd values of the microplasmas increase with increasing pressure and

discharge gap distance, the discharges exhibit more arc discharge characteristics as opposed to normal glow discharge characteristics. During this transformation from normal glow discharges to an arc discharges with increasing pressure, the discharges change from nonthermal to thermal discharges and two primary discharge characteristics change. The ionization method changes from electron impact ionization to thermal ionization, and the cathodes emit thermionic electrons as opposed to secondary electrons due to cathode heating.²⁶ Secondary electrons are the major source of ionization in microplasmas, and a reduction in the number of secondary electrons, which is associated with arc characteristics at higher pd values, affects the electron density and pressure removal rate of micro-SIPs.

The gas removal rates of micro-SIPs are affected by the composition of the exposed electrode pair surfaces. When reactively sputtering at high pressures, the chemical reactions occur directly on the cathodes surfaces.²⁷ In addition, the chemically active cathodes can become saturated over time, reducing the removal rates. Removal rates are also reduced by redeposition and the buildup of insulating films, such as TiO_2 , on the anode in a scenario termed the “disappearing-anode effect.” This scenario can cause changes in the metal impedance and arcing characteristics. This is especially characteristic at higher pressures, where large amounts of redeposition are encountered due to a small mean free path.²⁸ The buildup of positive charge due to positive ion bombardment on electrically insulated or poisoned portions of the cathodes can lead to arcing under dc operation as well. To reduce this effect, pulsed discharges can be used instead of dc discharges.

To predict the quantified gas removal rate of micro-SIPs, a model is reported here based on macroscale reactive sputtering models. Berg *et al.*^{29,30} and Li and Hsieh³¹ presented a model which considers the pressure change in a macroscale system as a function of target erosion, gas injection, reactive gas gettering at all surfaces, etc. The model determines the fractional coverage of a metal target and substrate by a compound film as they are sputtered by argon mixed with a reactive gas. The fractional surface coverage θ indicates the fraction of sites on the target surface occupied by the compound over the total number of target sites, while $(1 - \theta)$ indicates the fraction of unreacted metal sites. The change in the number of sites occupied by the compound on the target per unit time is expressed as

$$\frac{dN}{dt} = \alpha_m FA(1 - \theta)a - \frac{JS_N}{e} A\theta + \alpha_m FS_N A\theta a, \quad (1)$$

where F is the reactive gas flux, A is the target area, α_m is the sticking coefficient of the reactive gas molecules to the pure metal, a is the stoichiometric number of compound formation (ratio of compound molecules/reactive molecules), J is the ion current density, e is the unsigned charge of an electron, and S_N is the sputtering yield of the compound (atoms sputtered/incident atom). The first term in Eq. (1) represents the reaction between the reactive gas molecules and the fresh metal portion of the target. The second term represents the

reduction in compound fraction as a result of sputtering the compound off the metal. The third term represents the reaction between the reactive gas molecule and fresh metal sites which are uncovered when a compound molecule is sputtered.³² The reactive gas flux is determined using a Maxwellian distribution of molecular velocities as

$$F = \frac{p_p}{\sqrt{2\pi m k_B T}}, \quad (2)$$

where p_p is the partial pressure of the reactive gas, m is the mass of the reactive gas molecule, k_B is the Boltzmann constant, and T is the temperature. In this model, all of the absorbed reactive gas molecules are assumed to contribute to the formation of compound molecules on the target surface.

The macroscale model developed by Berg *et al.*^{29,30} describes reactive sputtering systems with low reactive gas partial pressures and requires adaptation to describe the high-pressure environments in which micro-SIPs are operated in this study. The primary difference between the two models is due to the high impingement rate of reactive gas molecules at high pressures, which impinge without sputtering. These molecules form native oxide, or other compound layers, covering the entire substrate surfaces. This leaves no fresh titanium to getter reactive molecules without sputtering. Theoretically, this can be confirmed by finding the critical pressure above which the target surface is completely covered by a compound. This critical pressure is determined by equating the rate at which the compound is removed by sputtering, the second term in Eq. (1), and the rate at which the compound is increased by reactive gas molecules impinging on the fresh metal sites, the third term in Eq. (2), and solving for the pressure to obtain the ratio

$$P_{\text{crit}} = \left(\frac{S_N J A}{e} \right) \left(\frac{(2\pi m k_B T)^{1/2}}{\alpha S_N a A} \right). \quad (3)$$

Using nitrogen as the reactive and sputtering gas, using a titanium cathode as the target, assuming stoichiometric TiN as the compound, and using other parameters determined from the micro-SIP design, the critical pressure is calculated as 1.98 Torr. Given that micro-SIPs are operated at pressures much higher than this, the entire surface is covered during normal operation. Considering the use of pure nitrogen as a reactive gas and given that the entire surface will be covered by TiN after the native oxide layer is removed, the removal of nitrogen gas only results from sputtering TiN molecules to expose fresh titanium atoms which will bond with the nitrogen. This indicates that the first term in Eq. (1) is irrelevant and the third term is the only relevant term indicating nitrogen removal from the environment and, consequently, pressure reduction. However, the process is now limited by the sputtering rate as opposed to the gas impingement rate, making the rate of nitrogen removal by the micro-SIPs simply

$$Q_{\text{pump}} = S_N^- A \theta. \quad (4)$$

This does not need to consider the sticking coefficient as available sites will be filled much faster than the rate at

which they are uncovered. TiN is considered to be sputtered as a molecule, as opposed to as titanium and nitrogen separately. As no fresh titanium is being sputtered from the cathode onto other portions of the substrate, all of the evacuated gas molecules are bound to the surface of the cathode, and not on other portions of the substrate.

The pressure reduction resulting from the removal of nitrogen from air is determined using the parameters below. By the ideal gas law, the change in pressure is

$$\frac{dp}{dt} = - \frac{k_B T}{V} S_N^- A \theta. \quad (5)$$

Considering a micro-SIP with a 50 μm discharge gap and 1500 V applied at a pressure of 100 Torr, 1.49×10^{14} molecules per second are sputtered and absorbed while the pressure changes by 68.6 mTorr/min. The rate at which nitrogen impinges on fresh titanium is

$$\frac{dN}{dt} = \alpha_m F S_N A \theta \quad (6)$$

and is equal to 5.2×10^{19} molecules per second. This is almost five orders of magnitude faster than the rate at which the surface is sputtered, indicating that the assumption of a sputter rate limited equation is valid.

Several parameters are required to calculate the gas removal rate of micro-SIPs using the above equations, including the stoichiometric number, the sticking coefficients, the sputtering yields, the electric field strengths, and the current density. The stoichiometric number used is 2, as two titanium atoms can bond with a single N_2 molecule. The sticking coefficient of nitrogen molecules on pure titanium is 0.4 at 20 °C and the sticking coefficient of N atoms on TiN_x films is ~ 0.003 for nitrogen-rich TiN films.³³ The sputtering yields, which are the number of atoms or molecules ejected from a target surface per incident ion, are calculated for nitrogen ions impinging on fresh titanium and TiN according to previously derived equations.²⁸ In a nitrogen dc discharge with higher current but lower current density, N_2^+ ions were found to have average energies of 100 eV in close proximity to the cathode.³⁴ These high-energy ions are created in the negative glow and undergo dissociative charge exchange in the cathode dark space to yield N^+ . Higher applied voltages also decrease the number of collisions for ions in the sheath, causing a larger number of high-energy ions.³⁵ Using an impinging ion energy of 100 eV, the sputtering yield of pure titanium is calculated as 0.14 while the combined yield of titanium and nitrogen from TiN is 0.24. A large number of ions have significantly less energy but are not considered in the calculation. The combined yield of titanium and nitrogen from TiN is typically larger than that of titanium from pure titanium, while the yield of just titanium from TiN is smaller than that of titanium from pure titanium.³⁶ Sputtering yields are typically very low at high pressures but are aided by the very localized plasmas in micro-SIPs.

COMSOL MULTIPHYSICS® FEA analysis of the described micro-SIP design, with 50 μm discharge gaps and an applied voltage of 1500 V, was used to simulate the experienced

TABLE I. Parameters for a micro-SIP with 50 μm discharge gaps and 1500 V applied at a pressure of 100 Torr.

Parameter	Value
First ionization coefficient α (cm^{-1})	761
Second ionization coefficient γ	2.47×10^{-7}
Current density (A/cm^2)	3.4×10^{16}
E/p [$\text{V}/(\text{cm Torr})$]	750
Sputtering rate and nitrogen consumed (molecules/s)	1.49×10^{14}
Nitrogen removal rate (mTorr/min)	68.6

electric fields above the micro-SIP electrodes. The analysis reveals uniform electric field strengths around the circular discharge gaps. It also reveals the arclike orientation of electric field lines, which indicates that the distance between electrodes, as experienced by the bombarding ions, is longer than the planar discharge gap separation. The theoretical distance is approximately four times the planar discharge gap spacing, and this increase in distance is included in the micro-SIP model to more accurately describe the ion trajectories. The resulting electric field intensity for this particular micro-SIP is 75 kV/cm, which is higher than traditional plasmas due to the small gap spacing.

The current density experienced by the ions is estimated as³⁷

$$J = \left(\frac{P}{C}\right) \frac{I}{A} \frac{1}{(1 + \gamma)}, \quad (7)$$

where γ is the secondary electron Townsend ionization coefficient, P is the pressure, and C is a correction factor. The pressure correction factor (P/C) is included to model the change in microplasma current density with pressure. A summary of parameters for the described micro-SIP is displayed in Table I.

V. EXPERIMENTAL AND MODELING RESULTS

A. Removing air from microelectronic packages

Micro-SIPs were sealed in industry-standard packages with pressure sensors and operated with externally applied voltages while the pressure was monitored. The three versions of the micro-SIPs described in Sec. III were used. They were hermetically sealed in metal flatpack packages, which are often used for power electronics. One package was a $3.3 \times 4.3 \text{ cm}^2$ (6.33 cm^3) gold plated nickel package from HCC Aegis (Catalog No. 0J7H2), while the second was a $2.5 \times 2.5 \text{ cm}^2$ (2.2 cm^3) steel package from Sinclair Manufacturing Co. (Product No. SQ 1000-250-12-10GC). Solder-bonded stainless steel lids were used to seal the packages. The pressure was measured by two piezoresistive pressure sensors (Freescale MPXH6115A) for confirmation in the larger package and by one in the smaller package. A multimeter and a computer interface were used to record the pressure sensor output voltages at programmable intervals while the current was also recorded.

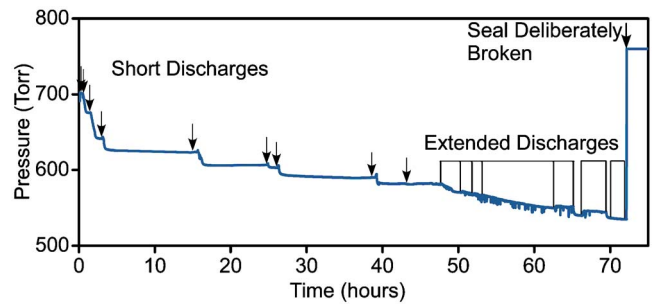


FIG. 4. Pressure drop in a 6.33 cm^3 package over time. Fifteen consecutive discharges drop the pressure 168 Torr. The pressure remains stable over periods of 10 h of micro-SIP inactivity and returns to atmospheric pressure when the package is opened.

The package pressures were reduced through micro-SIP operation. Three micro-SIPs were sealed in the 6.33 cm^3 package at atmospheric pressure. In one test demonstrating a typical amount of air removal, 15 discharges were applied to the micro-SIPs using four different electrode pairs, and the pressure was reduced by 168 Torr from the sealing pressure, as shown in Fig. 4. The pressure remained steady for periods of up to 10 h between discharges, and the figure shows that the pressure sensor correctly measured atmospheric pressure when the cavity was opened for inspection. Figure 5 displays the same pressure loss and absorbed molecules as a function of the energy used for the discharges. The upper trend line represents the pressure drops measured with the discharge off, when no energy was being applied to the system. In the 2.2 cm^3 package, the pressure has been reduced by 126 Torr through the application of extended discharges.

Some general trends concerning pulse duration and saturation were observed in all tests. Pulses of different durations produced varied pressure responses. Reactively sputtering for short periods, e.g., 10 min, resulted in pressure rises due to increases in temperature followed by sharp pressure declines as gases were chemisorbed. The pressure rose for approximately 3 of the 10 min before falling sharply. After

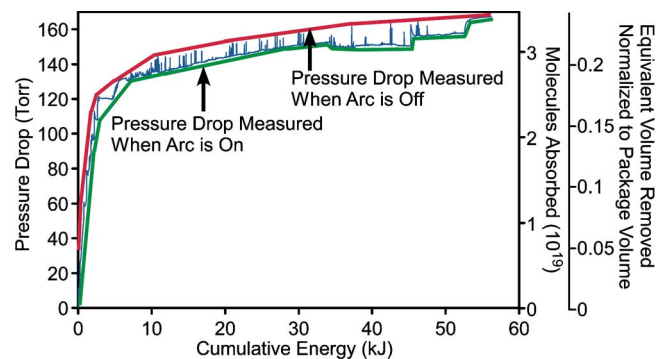


FIG. 5. Pressure drop, shown in Fig. 4, as a function of cumulative energy supplied to the discharge with an initial pressure of 760 Torr. The upper and lower trend lines, respectively, show the pressure readings when the discharge is interrupted (causing spikes as the pressure stabilizes without an increase in energy) and when the discharge remains on. The corresponding number of gas molecules removed at room temperature and the fraction of the package volume evacuated are noted on the second Y axis.

discharge extinction, the pressure continued to drop for up to 20 min and eventually stabilized, holding steady for hours between discharges. Reactively sputtering for extended durations, e.g., hours, resulted in steady pressure drops after initial rises due to temperature. To maintain discharges for hours, the applied voltages required increases with time due to the effective increase in discharge gap spacing as the proximal cathode regions were sputtered away.

The micro-SIPs showed signs of saturation when operated for long periods of time. For example, the initial discharge in Fig. 4 reduced the pressure by 678 mTorr/min, while the extended discharge reduced the pressure by 27 mTorr/min. This saturation is evident in all examined micro-SIPs and could have been caused by a lack of cathode material after a great deal was sputtered off, by a buildup of insulating nitride or oxide films, or by saturation of the cathode titanium which precluded absorption of more gases. However, temporarily reversing the electrode bias or using ac driven discharges may circumvent these restraints and will be pursued in future studies.

Opening the cavities revealed that titanium regions of the cathodes had been sputtered, as shown in Fig. 3(d). A film was also evident on the substrates and anodes. Areas of the 1 μm thick titanium were completely removed down to the glass substrate in the intended manner. As the titanium was sputtered from the initial discharge locations, the discharges occurred at different locations and thus sputtered the cathodes uniformly on all sides of the anodes. This uniform removal led to the concentric consumption of the cathodes over time. The anodes remained largely intact, showing no indication of sputtering, although some delamination and damage could potentially occur due to heating caused by current spikes.

B. Relationship between discharge gap spacing, pressure, and air removal rate

To determine the relationship between the micro-SIPs' gas removal rates, the initial ambient pressure, and the discharge gap spacing, micro-SIPs with varied discharge gaps were operated in air at different initial pressures. Version 2 micro-SIPs with identical designs and 1.82 mm² cathodes were used, having 35, 50, 75, 100, and 150 μm planar physical discharge gaps at pressures between 100 and 725 Torr in a 4 cm³ package. At these pressures all of the discharge gaps were much larger than the mean free path of gas molecules. The initial pressures inside the package were set using a mechanical pump.

The air removal rate varied as a function of pressure, discharge gap spacing, and discharge characteristics. Figure 6 shows the experimental and theoretically determined pressure removal rates as a function of starting pressure (P_s). The theoretical rates were calculated using the calculated removal rate of nitrogen in air. The theoretical model exhibits the same dependence of gas removal rate on pressure but overestimates the removal rate of large discharge gap micro-SIPs and underestimates the rate of smaller discharge gap micro-SIPs. In micro-SIPs with smaller discharge gaps, 35 and

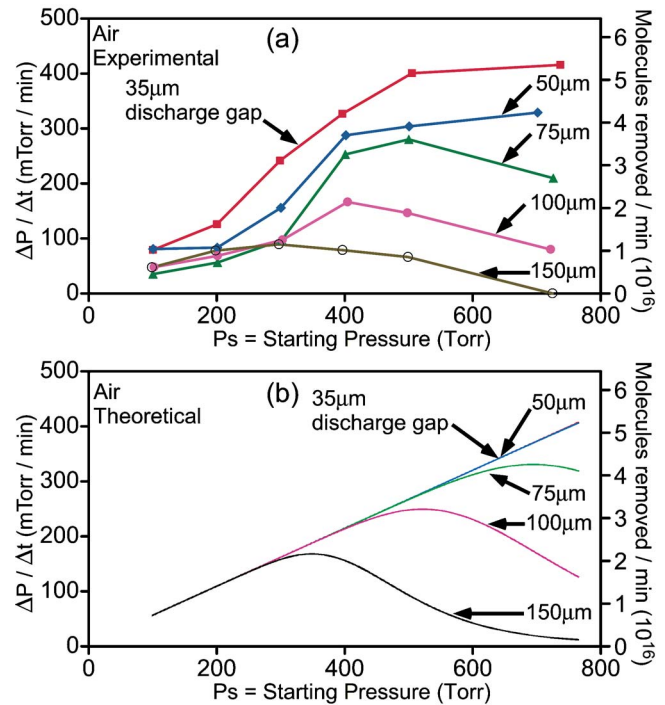


FIG. 6. (a) Experimentally measured (over 20 min) and (b) theoretically determined pressure removal rates of air as a function of discharge gap spacing and pressure. The micro-SIPs have between 35 and 150 μm discharge gaps, are operated with 1500 V, have initial pressures between 100 and 725 Torr, and are operated in a 4 cm³ package.

50 μm , higher initial pressures resulted in faster gas removal rates as a result of the increase in electron density, ionization, and secondary electron peak power at increasing pressures. At each examined pressure, micro-SIPs with smaller discharge gaps generally removed air faster than micro-SIPs with larger discharge gaps. This is consistent with the larger ionization coefficients and resulting increase in ionization and secondary electron production associated with smaller discharge gap micro-SIPs. A change in micro-SIP discharge characteristics, from normal glow discharges to arc discharges, was associated with a reduction in removal rate. As the starting pressure was increased for the micro-SIPs with larger discharge gaps, 75 μm and larger, the discharges became very spatially confined, the cathode spots meandered about the cathode surfaces, the discharges exhibited increasing arc characteristics, and the pressure reduction rates decreased. This decrease in pressure reduction rate with an increase in pressure in larger gap micro-SIPs caused the maximum pressure reduction rate of these micro-SIPs to occur at pressures less than atmosphere. The coinciding change in discharge characteristics and pressure reduction rate, as the gas pressure is increased, suggests that a reduction in secondary electron production in the arclike discharges causes the pumping rate to decrease.

C. Removal rate of various gases

Figure 7 shows the species being ionized and excited in an air environment at 760 Torr, as identified by examining

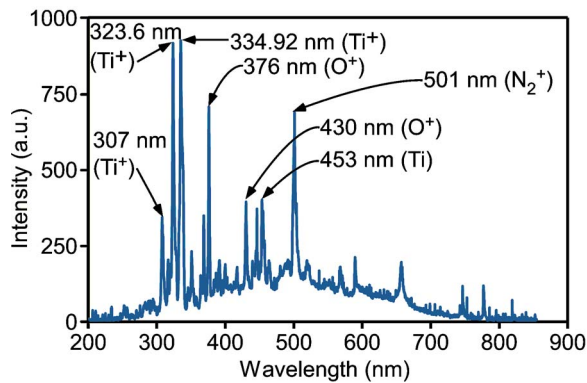


FIG. 7. Spectrum of the micro-SIP electrode pair discharge in air indicating the dissociation of oxygen and ionization of titanium and nitrogen.

the spectrum produced by the discharge.^{38,39} In this mixed gas environment, the strongest emissions are produced by Ti^+ , O^+ , and N_2^+ . The gas selectivity of titanium micro-SIPs was examined by individually introducing pure nitrogen, oxygen, and helium (as an inert reference) into a previously evacuated package and measuring the removal rates at 200 Torr. The version 2 micro-SIP design with 1.82 mm^2 cathodes and $100 \mu\text{m}$ discharge gaps was used. Figure 8 illustrates the pressure removed in each environment; oxygen is removed faster than nitrogen, and helium is not noticeably removed. Helium is not removed as it is an inert gas and does not bond with titanium. Averaging three trials, oxygen is found to be removed at 11.5 Torr/h , nitrogen at 3.4 Torr/h , and air at 7.2 Torr/h . Oxygen is removed at over three times the rate of nitrogen, which corresponds to the ratio of chemisorption rates of these gases on titanium at room temperature.⁹ This suggests that in a mixed gas environment such as air, oxygen will be removed more rapidly than nitrogen as well. This was experimentally confirmed, as shown in Fig. 8.

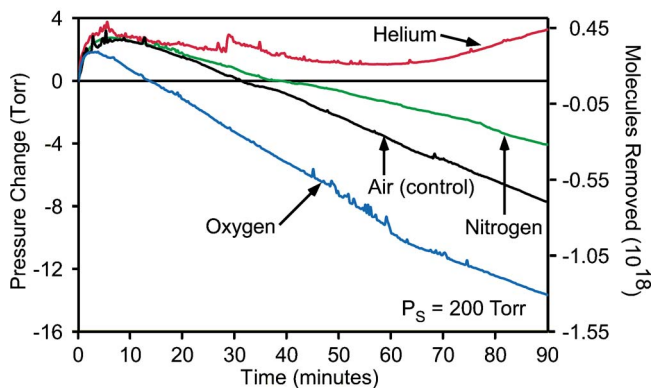


FIG. 8. Change in pressure in environments of pure oxygen, nitrogen, helium, and air. The micro-SIPs have $100 \mu\text{m}$ discharge gaps, are operated with 1000 V, have initial pressures of 200 Torr, and are operated in a 4 cm^3 package. This shows that the mixed gas air environment is removed at a rate between oxygen and nitrogen as expected, based on the different chemisorption rates of the gases. Helium is not removed as it is an inert gas and does not bond to titanium.

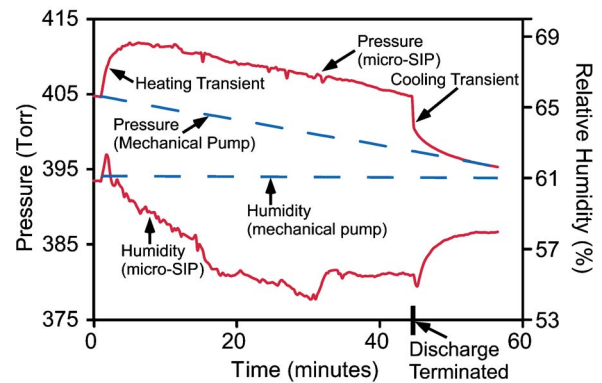


FIG. 9. Experimentally measured change in humidity observed using a micro-SIP. The micro-SIP has a $100 \mu\text{m}$ discharge gap, is operated with 1000 V, has an initial pressure of 400 Torr, and is operated in a 0.33 cm^3 ceramic package. A mechanical pump is used for comparison, starting at the same initial pressure and relative humidity. The micro-SIP removes more relative humidity than the mechanical pump when both remove 10 Torr. The heating and cooling transients are caused by the discharge induced heat from the micro-SIP. They are absent in the mechanical pump measurements due to the absence of a heat increase.

D. Removal rate of water vapor

The ability of micro-SIPs to remove water vapor was determined by introducing water vapor into sealed packages and measuring the relative humidity drop during micro-SIP operation with humidity sensors. Figure 9 shows the typical relative humidity and pressure drops observed using a version 2 micro-SIP with a $100 \mu\text{m}$ discharge gap at a starting pressure of 400 Torr. For comparison, it also shows the relative humidity drop when a mechanical pump was used to remove the same amount of pressure from the same package. A micro-SIP removed 4% relative humidity while reducing the pressure by 10 Torr in 45 min. Using the mechanical pump to remove 10 Torr, starting from the same initial pressure and relative humidity, reduced the relative humidity by only 0.1%. Initially, the micro-SIP removed humidity much faster than the mechanical pump over the same pressure drop, but this measurement was influenced by the temperature increase while the discharge is on, which caused a lower relative humidity reading. After the micro-SIP was turned off, the relative humidity rose and stabilized at a value lower than that obtained simply by removing the air with the mechanical pump. This indicates that micro-SIPs can operate effectively in the presence of water vapor and may offer an advantage to mechanical pumps in the suppression of humidity.

E. Pulsed discharge operation

To evaluate the removal rate improvements possible through the reduction of positive charge buildup on the cathodes, and possible energy efficiency improvements, pulsed discharges were applied to version 2 micro-SIPs with $50 \mu\text{m}$ discharge gaps at an initial pressure of 400 Torr in a 4 cm^3 package. Figure 10(a) shows the removal rates obtained when the current applied to the micro-SIPs was pulsed for periods between 25 and 500 ms, at a frequency of 1 Hz. The

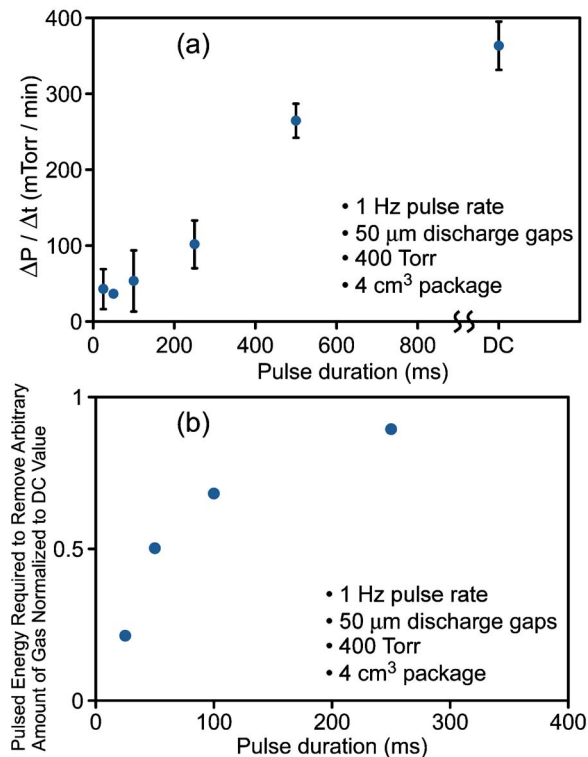


FIG. 10. (a) Pressure removal rate as a function of pulse duration, averaged over 20 min of gas removal. Pulses of 1000 V are all applied at a frequency of 1 Hz. The longer pulse durations remove pressure faster. The error bars indicate a standard deviation of removal rate. (b) Relative energy required to remove an arbitrary unit of pressure with different pulse durations, normalized to a dc discharge. This indicates that micro-SIPs utilizing short pulses remove almost five times as much pressure as micro-SIPs utilizing dc discharges when the same amount of energy is applied.

rate at which air was removed from the package was directly related to the duration of this applied current. Micro-SIPs operated using dc discharges removed air faster than pulsed discharges with duty cycles of 50% or less, showing that pulsing compromises evacuation rates. Figure 10(b), however, compares the relative energy required by micro-SIPs using pulsed discharges of different durations to remove a fixed amount of air from a package. The energy required to remove this arbitrary amount of air with the different duration discharges is normalized to the amount of energy required by a dc discharge. This indicates that given the same amount of energy and enough time to apply this energy to pulsed discharges at a set frequency, micro-SIPs using pulses of 25 ms in duration can remove almost five times as much air as micro-SIPs using dc discharges. This also indicates that shorter pulses are more energy efficient despite their slower removal rates as they are able to dissipate charge buildup on the electrodes. Pulsed discharges also increased electrode lifetime, probably as a result of a reduced thermal load on the cathode.

VI. CONCLUSION

This effort explores the use of microscale titanium sputter-ion pumping using pulsed and dc microdischarges be-

tween thin-film electrodes. The micro-SIPs function in sealed cavities without heating surrounding devices and provide control over the amount of air and humidity removed from the inside of the cavity. In an air environment, these devices remove 168 Torr from a 6.33 cm³ cavity and 126 Torr from a 2.2 cm³ cavity when starting at an atmospheric pressure. The gas removal rates depend on both the initial pressure and discharge gap spacing. Micro-SIPs with smaller discharge gaps operating at higher initial pressures remove air at the greatest rate. This relationship qualitatively matches analytical estimates. Oxygen, nitrogen, and air are removed at rates of 11.5, 3.4, and 7.2 Torr/h, respectively, at 200 Torr while helium is not removed. Water vapor is removed from a sealed package at a rate of 6% relative humidity per hour. Using pulsed discharges, a five times increase in power efficiency is achieved per molecule removed. These data concerning the operation and characteristics of micro-SIPs suggest that they are promising for low-temperature control of vacuum-sealed packages in microelectromechanical system applications.

ACKNOWLEDGMENTS

The authors are grateful for the assistance received from B. Mitra and K. Tan and for the fabrication work of J. Park and W. Zhu. This work was supported primarily by the Engineering Research Center Program of the National Science Foundation under Award No. EEC-9986866. The facilities used for this research include the Michigan Nanofabrication Facility (MNF) at the University of Michigan.

- ¹H. Guckel and D. W. Burns, U.S. Patent No. 4, 744,863 (17 May 1988).
- ²H. Henmi, S. Shoji, Y. Shoji, K. Yoshimi, and M. Esashi, *Sens. Actuators, A* **43**, 243 (1994).
- ³H. J. Halama and Y. Guo, *J. Vac. Sci. Technol. A* **9**, 2070 (1991).
- ⁴D. R. Sparks, S. Massoud-Ansari, and N. Najafi, *IEEE Trans. Adv. Packag.* **26**, 277 (2003).
- ⁵St707 Getter Alloy for Vacuum Thermal Insulation, <http://www.saesgetters.com/default.aspx?idpage=273>
- ⁶J. Hobson and D. Salzman, *J. Vac. Sci. Technol. A* **18**, 1758 (2000).
- ⁷S. McNamara and Y. B. Gianchandani, *J. Microelectromech. Syst.* **14**, 741 (2005).
- ⁸K. M. Welch, *J. Vac. Sci. Technol. A* **21**, S19 (2003).
- ⁹L. Holland, *J. Sci. Instrum.* **36**, 105 (1959).
- ¹⁰D. M. Mattox, *Plat. Surf. Finish.* **88**, 74 (2001).
- ¹¹D. R. Denison, *J. Vac. Sci. Technol.* **4**, 156 (1967).
- ¹²B. F. Coll and M. Chhowalla, *Surf. Coat. Technol.* **68-69**, 131 (1994).
- ¹³E. Barborini, P. Piseri, and P. Milani, *J. Phys. D* **32**, L105 (1999).
- ¹⁴D. B. Go, S. V. Garimella, and T. S. Fisher, Tenth Intersociety Conference on Thermal and Thermomechanical Phenomena and Emerging Technologies in Electronic System, San Diego, CA, 30 May–2 June 2006, p. 45.
- ¹⁵S. A. Wright and Y. B. Gianchandani, *IEEE/ASME International Conference on Micro Electro Mechanical Systems (MEMS 06)*, Istanbul, Turkey, 22–26 January 2006, p. 754.
- ¹⁶C. G. Wilson, Y. B. Gianchandani, R. R. Arslanbekov, V. Kolobov, and A. E. Wendt, *J. Appl. Phys.* **94**, 2845 (2003).
- ¹⁷M. J. Kushner, *J. Phys. D* **38**, 1633 (2005).
- ¹⁸C. G. Wilson and Y. B. Gianchandani, *J. Microelectromech. Syst.* **10**, 50 (2001).
- ¹⁹C. G. Wilson and Y. B. Gianchandani, *IEEE/ASME International Conference on Micro Electro Mechanical Systems (MEMS 04)*, Maastricht, The Netherlands, 25–29 January 2004, p. 765.
- ²⁰C. G. Wilson and Y. B. Gianchandani, *IEEE Trans. Plasma Sci.* **32**, 282 (2004).
- ²¹B. Mitra and Y. B. Gianchandani, *IEEE Conference on Sensors*, Irvine,

- CA, 30 October–3 November 2005, p. 326.
- ²²R. Foest, M. Schmidt, and K. Becker, *Int. J. Mass. Spectrom.* **248**, 87 (2006).
- ²³A. Vesel, M. Mozetic, and A. Zalar, *Appl. Surf. Sci.* **246**, 126 (2005).
- ²⁴J. D. Cobine, *Gaseous Conductors Theory and Engineering Applications* (Dover, New York, 1941), Vol. 1, p. 160.
- ²⁵Y. P. Raizer, *Gas Discharge Physics* (Springer, Berlin, 1991), Vol. 1, pp. 52, 128, and 324.
- ²⁶D. Staack, B. Farouk, A. Gutsol, and A. Fridman, *Plasma Sources Sci. Technol.* **14**, 700 (2005).
- ²⁷M. Madou, *Fundamentals of Microfabrication: The Science of Miniaturization*, 2nd ed. (CRC, Boca Raton, FL, 2002), Vol. 1, p. 140.
- ²⁸M. Ohring, *The Materials Science of Thin Films* (Academic, San Diego, CA, 1992) Vol. 1, pp. 111 and 120.
- ²⁹S. Berg, H.-O. Blom, T. Larsson, and C. Nender, *J. Vac. Sci. Technol. A* **5**, 202 (1987).
- ³⁰S. Berg, T. Larsson, C. Nender, and H.-O. Blom, *J. Appl. Phys.* **63**, 887 (1988).
- ³¹C. Li and J. Hsieh, *Thin Solid Films* **475**, 102 (2005).
- ³²M. Yoshitake, K. Takiguchi, Y. Suzuki, and S. Ogawa, *J. Vac. Sci. Technol. A* **6**, 2326 (1988).
- ³³K. Yokota, K. Nakamura, T. Kasuya, K. Mukai, and M. Ohnishi, *Thin Solid Films* **473**, 340 (2005).
- ³⁴S. Kumar and P. K. Ghosh, *Int. J. Mass Spectrom. Ion Process.* **127**, 105 (1993).
- ³⁵S. Peter, R. Pintaske, G. Hecht, and F. Richter, *J. Nucl. Mater.* **200**, 412 (1993).
- ³⁶R. Ranjan, J. P. Allain, M. R. Hendricks, and D. N. Ruzic, *J. Vac. Sci. Technol. A* **19**, 1004 (2001).
- ³⁷S. Zhu, F. Wang, and W. Wu, *J. Appl. Phys.* **84**, 6399 (1998).
- ³⁸G. R. Harrison, *Massachusetts Institute of Technology Wavelength Tables* (MIT, Cambridge, MA, 1969) Vol. 1, pp. 98, 132, 155, 218, 274, 289, and 309.
- ³⁹R. W. B. Pearse, *The Identification of Molecular Spectra*, 3rd ed. (Chapman and Hall, London, 1963), Vol. 1, pp. 176 and 197.